JOURNAL OF MATERIALS SCIENCE 31 (1996) 345–349

A microstructural investigation of NiAl/Ni–Si–B/NiAl transient liquid phase bonds

W. F. GALE, S. V. OREL
Materials Research and Education Center, Auburn University, Auburn, AL 36849, USA

Microstructural development during transient liquid-phase bonding of cast polycrystalline near-stoichiometric NiAl (B2 compound, β-phase) was investigated using cross-sectional transmission electron microscopy. Bonds made using Ni–4.5 wt% Si–3.2 wt% B (AWS designation BNi-3) interlayers in the form of melt-spun foils were studied. Microstructural changes in the joint region and surrounding substrates were examined as a function of holding time at temperatures of 1065 and 1150 °C. The transformation of the substrate β-phase to $L1_0$-type martensite due to aluminium transfer to the joint has been discussed, and the formation of $L1_2$ type (γ′ structure) layers at the joint–substrate interfaces considered. The nature of the isothermal solidification process has also been discussed and the changes, with holding time at the bonding temperature, in the character of the residual eutectic examined. The formation of $M_{23}X_6$-type borides within both the joint and surrounding substrates was also considered.

1. Introduction

The B2-type intermetallic compound NiAl (β-phase) has attracted considerable interest as a candidate material for high-temperature structural applications (e.g. [1–3]). However, joining technologies appropriate to NiAl will be required if this intermetallic is to achieve its full potential as a structural material [4]. Transient liquid-phase (TLP) bonding (e.g. [5, 6]) is compatible with the strong alumina-forming tendency and poor low-temperature ductility/toughness of NiAl.

TLP bonding of NiAl has formed the subject of a number of recent investigations (e.g. [7, 8]). These studies have considered the use of interlayer materials (such as pure nickel) that are suited to NiAl–NiAl joining, rather than joining of NiAl to lower melting-point materials such as conventional nickel-base alloys. The present work represents part of an investigation of the joining of NiAl to nickel-base alloys using Ni–4.5 wt% Si–3.2 wt% B interlayers (AWS designation BNi-3). The BNi-3 interlayers have a relatively low liquidus temperature of 1040 °C [9] and Ni–Si–B-based materials are suitable for joining of nickel-base alloys [10].

The present paper reports microstructural development in NiAl–NiAl bonds made with the BNi-3 interlayer. The intention of the work was to provide a microstructural reference that can be used to aid understanding of microstructural development in relatively complex NiAl–Ni-base alloy joints. The paper considers both evolution of joint microstructures and the influence of the TLP bonding process on the surrounding NiAl substrate material.

2. Experimental procedure

TLP bonds were prepared between near stoichiometric cast NiAl (Ni–48 at %Al) substrates with a grain size of around 150 μm. Prior to bonding, the substrate materials were homogenized at a temperature of 1300 °C for 50 h. The TLP bonds employed 51 μm thick melt-spun interlayers of a Ni–4.5 wt% Si–3.2 wt% B alloy (AWS designation BNi-3). Bonding was conducted utilizing holding periods ranging between 0 (heating only) and 72 h at temperatures of 1065 and 1150 °C under a 10^{-4} mbar vacuum. Further details of bonding procedures may be found elsewhere [11].

Microstructural observations were made on cross-sectional samples using light microscopy (LM), scanning electron microscopy (SEM), and transmission electron microscopy (TEM) together with SEM- and TEM-based energy dispersive X-ray spectroscopy (EDS). Samples for LM and SEM were prepared by electrolytic etching at 3 V in a solution consisting of 30 vol % acetic acid, 30 vol % lactic acid, 20 vol % hydrochloric acid, 10 vol % nitric acid and 10 vol % distilled water. SEM examination was conducted using a JEOL 840 instrument operated at an accelerating voltage of 20 kV. TEM specimens were prepared by ion milling using argon ions generated using dual guns operating at 5 kV with gun currents of 500 μA per gun and gun–specimen angles of 15°. TEM was conducted using a JEOL 1200 EX microscope operated at an accelerating voltage of 120 kV. SEM- and TEM-based EDS employed a Tracor-Northern 5500 analyser attached to the JEOL 1200 EX and 840 instruments.

3. Results and discussion

Similar results were generally obtained with the 1065 and 1150 °C bonding temperatures. In the discussion below, attention is concentrated on the 1065 °C bonding temperature and differences with the 1150 °C bonding temperature are considered when present.

In the absence of a substrate material [12], the BNi-3 foil examined in the present investigation solidifies to form a γ(A1-type phase, nominally nickel) plus Ni_3B (cementite structured phase) eutectic mixture. Frequently, the γ-phase component of the eutectic will contain Ni_3Si (an $L1_2$-type phase that is isostructural with Ni_3Al) precipitates with a cuboidal morphology. These Ni_3Si precipitates form a cube–cube orientation relationship to the γ-phase. Proeutectic γ can be observed in some resolidified BNi-3 foils.

In the present investigation, the resolidified liquid present in NiAl/BNi-3/NiAl bonds given short holding-times (e.g. 0–3 min) at a bonding temperature of 1065 °C resembled that formed in the absence of a substrate. In these short holding-time bonds, the main effect of the presence of the NiAl substrates was found to be the formation of a layer of γ' ($L1_2$-type phase) at the interface between each substrate and the resolidified interlayer (the location of the γ' layers is shown schematically in Fig. 1). These γ' layers were found to be rich in both aluminium (originating from the substrates) and silicon (originating from the interlayer). The γ' layers were found to consist of $Ni_3(Al, Si)$ rather than distinct Ni_3Al and Ni_3Si phases.

The γ' layers were polycrystalline and consisted of columnar grains with boundaries oriented roughly perpendicular to the faying surfaces. The length of these columnar grains was typically around 2–5 μm. In general, the short axes of the columnar grains extended right across the γ' layer (which had a width of around 1 μm). The size of the columnar grains was far smaller than that of the NiAl substrates (typically around 150 μm) and no orientation relationship was noted between the γ' layers and the substrate β-phase. Isothermal solidification usually proceeds by epitaxial growth of the solid phase from the substrates into the joint. Furthermore, β/γ' orientation relationships of the Kurdjumov–Sachs type are observed in directionally solidified bulk intermetallics [13, 14]. Hence, the absence of a β/γ' orientation relationship in the TLP bonds considered in the present investigation would seem to be more consistent with precipitation of the γ' on cooling, rather than during isothermal solidification.

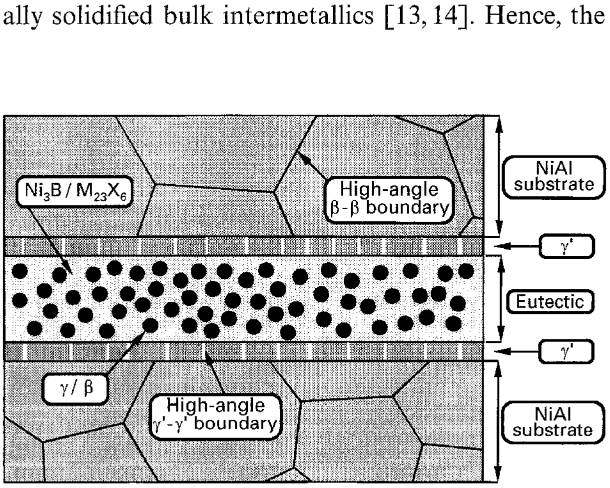

Figure 1 Schematic drawing showing the location of γ' and other microstructural features present during the early stages of bonding.

In samples subjected to prolonged holding (e.g. 2 h and above) at a bonding temperature of 1065 °C the formation of γ' layers at the joint–substrate interfaces was no longer observed. The absence of the γ' layer correlated with the entry of sufficient aluminium into the joint to result in the formation of the β-phase within the joint (as discussed below).

Aluminium diffusion into the (initially aluminium-free) joint correlated with the formation of an aluminium-depleted zone in the NiAl substrates immediately adjacent to the joint (see [15] for detailed compositional profiles). In samples subjected to intermediate holding times, this aluminium depletion was sufficient to result in martensitic transformation of the substrate β-phase. $L1_0$-type martensitic layers with widths of around 5–10 μm were observed within the NiAl substrates of bonds prepared using 2 h holding at 1065 °C. In contrast, martensite formation was not observed in samples subjected to either shorter or longer holding times (due respectively to a low extent of aluminium transfer from the substrate to the joint and removal of the aluminium-depleted zone by diffusion of aluminium from the bulk NiAl substrates). In bonds prepared at 1150 °C, aluminium transfer from the bulk substrates to the joint region was sufficiently rapid to prevent the formation of marked aluminium depleted zones. Hence, the formation of martensitic layers, within the ingrowing β-phase, was not observed in samples bonded at 1150 °C.

Aluminium diffusion from the NiAl substrates into the joint was found to modify substantially the character of the eutectic formed in joints cooled back to room temperature before the completion of isothermal solidification. At the nickel-rich end of the Ni–B binary system, the equilibrium boride phase is Ni_3B (e.g. [16]). However, an $M_{23}X_6$-type equilibrium phase with a nominal composition $Ni_{20}Al_3B_6$ appears within the Ni–Al–B ternary system [17]. These changes in equilibrium boride phase were mirrored in the NiAl/Ni–Si–B/NiAl bonds. Similarly, as the aluminium content of the joint region increased with holding time at the bonding temperature, a tendency was observed for the replacement of the γ-constituent of the eutectic by aluminium-rich phases. Thus, the following sequence of eutectic microstructures was observed in samples cooled back to room temperature:

1. a lamellar mixture of γ and Ni_3B (Fig. 2), also some regions comprised of γ spheres contained within Ni_3B blocks (initial condition);
2. spherical γ and Ni_3B in a matrix of $M_{23}X_6$, plus some regions consisting of angular Ni_3B in $M_{23}X_6$ (sample held for 20 min at 1065 °C);
3. spherical $L1_0$ martensite deposits in an $M_{23}X_6$ matrix (Figs 3 and 4; samples held for 120 min at 1065 °C or 20 min at 1150 °C);
4. spherical β-phase within an $M_{23}X_6$ matrix (samples held for longer than 120 min at 1065 °C).

In contrast, no evidence was found for the formation of $L1_2$-type phases within the eutectic.

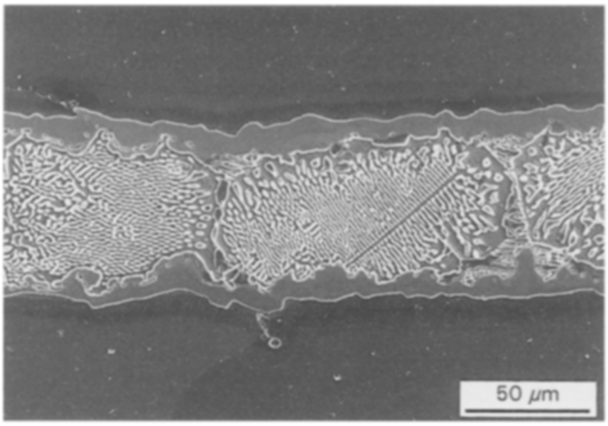

Figure 2 Secondary electron image showing the γ + Ni_3B eutectic formed during the early stages of bonding (sample held for 20 min at 1065 °C).

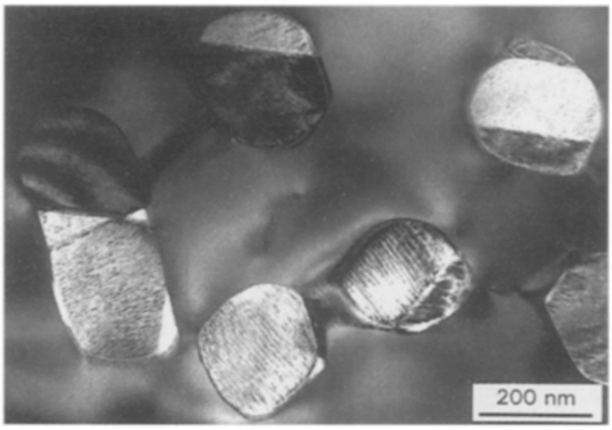

Figure 4 Bright-field micrograph showing spheroidal $L1_0$ martensite (produced by transformation of the β-phase constituent of the eutectic) surrounded by $M_{23}X_6$ at the centre-line of a bond held for 2 h at 1065 °C.

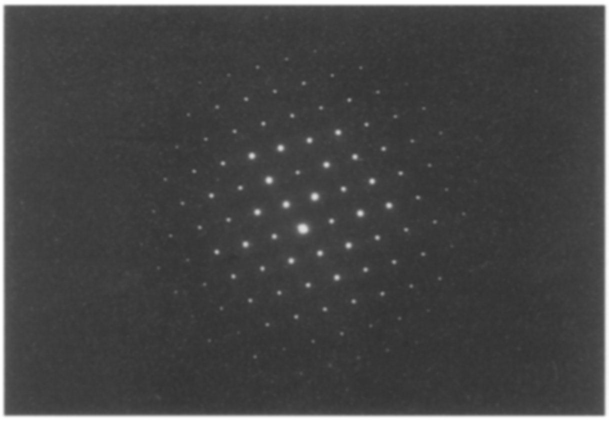

Figure 3 Selected-area diffraction pattern (beam direction $[1\,1\,0]_{M_{23}X_6}$) identifying $M_{23}X_6$ borides at the centre-line of a bond held for 20 min at 1150 °C.

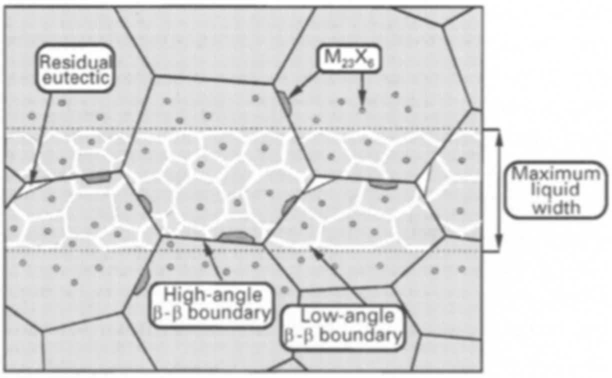

Figure 5 Schematic drawing showing the formation of low-angle β–β boundaries within the ingrowing β-phase and other features present during the later stages of bonding.

Isothermal solidification of the NiAl/Ni–Si–B/NiAl bonds proceeded by the epitaxial growth, into the joint, of the substrate β-phase. Thus, the grain size of the ingrowing β-phase was similar to that in the bulk NiAl substrates. However, a tendency was observed for the formation of sub-grains within the ingrown β-phase grains (as is shown schematically in Fig. 5). These subgrains were visible throughout the ingrown β-phase. Nonetheless, it is unclear as to whether the exact point of first appearance of the sub-grains was at, or immediately behind, the growing β-phase front. Typically the sub-grains had diameters of around 10 μm or less and were separated by low-angle boundaries generally with misorientations of less than 3°.

Markham [18] has observed premature recrystallization of oxide dispersion strengthened (ODS) nickel-base alloy substrates surrounding boron-containing TLP bonds. Markham suggested that, given that the boron atom is larger than the available interstitial sites in γ-Ni, the boron flux emanating from the TLP bonds stores sufficient strain energy in the γ-phase to promote recrystallization. By analogy, a possible explanation for the formation of the low-angle boundaries observed in the present work is boron-induced recovery of the β-phase. However, it should be noted that the ODS materials investigated by Markham were heavily cold-worked and hence had a large initial driving force for recrystallization. In contrast, such a driving force was not present in the bonds investigated in the present work, which were isothermally resolidified by epitaxial growth of β-phase from annealed NiAl substrates. Thus, the origins of the apparent occurrence of a recovery-like process within the joint region of the NiAl–NiAl bonds require further investigation.

The holding time required to complete isothermal solidification of the NiAl/Ni–Si–B/NiAl bonds varied markedly with lateral position in the joint. This variability in isothermal solidification time correlated with the occurrence of a cellular mode of isothermal solidification and, more particularly, with collection of liquid at β–β boundaries of the ingrowing solid. The resulting formation of a non-planar isothermal solidification front was of the greatest significance (with respect to the time taken to complete isothermal solidification) when the retarded regions of the solidification fronts growing from the two substrates happened to coincide. In these coincident regions, isothermal solidification was only completed after 72 h holding at 1065 °C whereas the remainder of the joint was isothermally solidified after 21 h holding at 1065 °C.

Precipitation of borides was observed within the β-phase matrix of both the isothermally resolidified portion of the joints and the substrates. Although the extent of boride precipitation increased with holding time at the bonding temperature of 1065 or 1150 °C, the character of the borides was similar under all conditions examined. The borides were found to be $M_{23}X_6$-type phases (for which M was mostly nickel with traces of aluminium, and X may be presumed to represent boron). Regardless of the location of the $M_{23}X_6$ precipitation (i.e. within the eutectic, ingrown β-phase or the substrates) the following orientation relationship was invariably observed between the β and $M_{23}X_6$ phases:

$$[0\,0\,1]_\beta \parallel [1\,1\,0]_{M_{23}X_6}$$

$$(1\,0\,0)_\beta \parallel (\bar{1}\,1\,1)_{M_{23}X_6}$$

When $M_{23}X_6$ precipitated intragranularly, a polygonal morphology was typically observed. In general, the polygonal $M_{23}X_6$ precipitates had diameters in the range 50–200 nm. $M_{23}X_6$ also precipitated on β–β boundaries (both low- and high-angle) with an angular morphology. Commonly, these grain-boundary precipitates extended about 1 μm along the boundary and around 100–400 nm into one of the adjacent (sub-) grains.

In Ni/Ni–Si–B/Ni joints, Gale and Wallach previously provided experimental evidence for the formation of Ni_3B- and $M_{23}X_6$-type borides at the bonding temperature after complete melting of the filler [19]. Direct evidence for the formation of Ni_3B at the bonding temperature was obtained by correlation of hot-stage X-ray diffraction with room-temperature TEM. The volume fraction of $M_{23}X_6$ was insufficiently large to permit detection of this phase by X-ray diffraction. Instead (as is described below), indirect evidence was obtained for the formation of $M_{23}X_6$ at the bonding temperature.

Extensive pinning of substrate (γ-phase) grain boundaries by $M_{23}X_6$ was observed following bonding in the Ni/Ni–Si–B/Ni system, thus implying that $M_{23}X_6$ precipitates were present during a period of significant γ grain growth.

Thermal exposure during the heating and cooling stages was minimized by using high heating and cooling rates. Thus, conditions compatible with the occurrence of grain growth were only present during holding at the bonding temperature. Furthermore, the depth of the γ grain-boundary pinning increased with holding time at the bonding temperature. Hence, the observation of pinning of the γ grain boundaries by $M_{23}X_6$ indicates that this boride phase was present at the bonding temperature. Given that $M_{23}X_6$ was not detected in samples heated to the bonding temperature and immediately cooled back to room-temperature, $M_{23}X_6$ could not have been formed during heating to the bonding temperature. Thus, the $M_{23}X_6$ would appear to have precipitated at the bonding temperature. $M_{23}X_6$ precipitated in this fashion was confined to the nickel substrates and did not appear within the proeutectic γ-Ni phase (the origins of this situation have been discussed in detail elsewhere [19]).

In the present investigation of NiAl/Ni–Si–B/NiAl bonds, significant growth in the β-phase grain size was observed after bonding. For example, after 21 h holding at a bonding temperature of 1065 °C, the grain size in the substrate β-phase had risen to about 200 μm, compared to around 150 μm before bonding. Nonetheless, despite the extensive presence of $M_{23}X_6$ on β-grain boundaries in NiAl/Ni–Si–B/Ni bonds cooled back to room temperature, no evidence was found for pinning of the β grain boundaries by $M_{23}X_6$. Furthermore, the extent of $M_{23}X_6$ precipitation in the β-phase decreased in a uniform fashion with increasing distance from the joint centre line. Hence, for example, in Fig. 6, no discontinuity is visible in the distribution of $M_{23}X_6$ corresponding to the interface between the substrate and ingrowing β-phase. Thus, unlike Ni/Ni–Si–B/Ni joints, the distribution of $M_{23}X_6$ in NiAl/Ni–Si–B/NiAl bonds is consistent with that expected from the precipitation of $M_{23}X_6$ on cooling to room temperature (for which boride precipitation should decrease in a uniform fashion with increasing distance from the boron source at the joint centre-line).

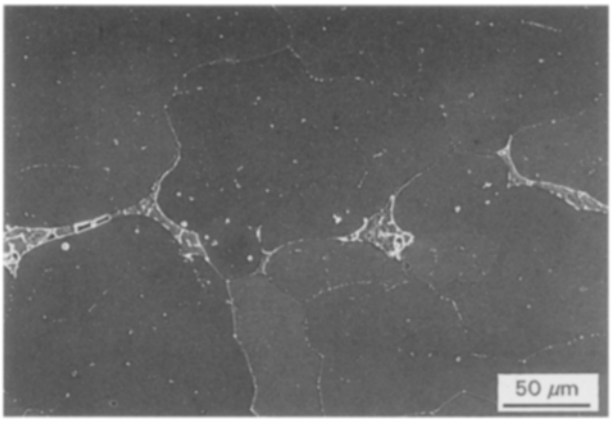

Figure 6 Secondary electron image showing residual eutectic and substrate borides in a bond held for 21 h at 1065 °C.

4. Conclusions

An investigation has been undertaken of microstructural development in transient liquid-phase bonds in the NiAl/BNi-3/NiAl system. This investigation has led to the following conclusions.

1. A layer of $L1_2$-type γ′, containing both aluminium and silicon, was formed at the interface between the initially aluminium-free eutectic and the Ni–48 at % Al β-phase substrates. The γ′ layer was not orientation related to either the substrate β-phase or constituents of the eutectic and appeared to have precipitated during cooling from the bonding temperature. Aluminium diffusion from the bulk substrates to the joint during bonding prevented the formation of the γ′ layer in isothermally resolidified samples.
2. Depletion of aluminium from the NiAl substrates by diffusion into the joint led to the formation of $L1_0$-type martensite in the β-phase surrounding the eutectic. An aluminium-depleted region, in which $L1_0$ martensite formation occurred, was only observed after intermediate bonding times (e.g. 2 h at 1065 °C) and not after longer or shorter holding periods.
3. Transfer of aluminium from the bulk substrates resulted in changes, with holding time at the bonding

temperature, in the nature of the eutectic produced on cooling. The following sequence of eutectic microstructures was observed with increasing holding time at the bonding temperature: (1) γ-Ni plus Ni_3B, (2) γ-Ni with Ni_3B and $M_{23}X_6$, (3) $L1_0$ martensite plus $M_{23}X_6$, and (4) β-phase with $M_{23}X_6$.

4. Isothermal solidification of the NiAl/Ni–Si–B/NiAl joints occurred by the epitaxial growth of nickel-rich β-phase into the joint. However, a tendency was observed for the formation of sub-grains within the epitaxially ingrown β-phase.

5. $M_{23}X_6$ precipitation was observed both within the substrate β-phase surrounding the joints and in the isothermally resolidified portion of the bonds. The observed distribution of $M_{23}X_6$ was consistent with precipitation of this phase on cooling from the bonding temperature.

Acknowledgements

The authors thank Dr Easo George, Oak Ridge National Laboratory, for the provision of the NiAl substrate material, and Mr Thomas Edwards, Allied Signal, for supply of the BNi-3 insert metal. Partial funding for the work was provided by the Oak Ridge Associated Universities organisation.

References

1. I. BAKER and P. R. MUNROE, in "High Temperature Aluminides and Intermetallics", edited by S. H. Whang, C. T. Liu, D. P. Pope and J. O. Stiegler (TMS, Warrendale, PA, 1990) pp. 425–52.
2. S. NAKA, M. THOMAS and T. KHAN, *Mater. Sci. Technol.* **8** (1992) 291.
3. K. VEDULA and J. R. STEPHENS, *MRS Symp. Proc.* **81** (1987) 381.
4. D. M. DIMIDUK, D. B. MIRACLE and C. H. WARD, *Mater. Sci. Technol.* **8** (1992) 367.
5. D. S. DUVALL, W. A. OWCZARSKI and D. F. PAULONIS, *Weld. J.* **53** (1974) 203.
6. W. A. OWCZARSKI, in "*Physical Metallurgy of Metal Joining*", edited by R. Kossowsky and M. E. Glicksman (Metallurgical Society of AIME, Warrendale, PA, 1980) pp. 166.
7. M. J. STRUM and G. A. HENSHALL, "Advanced Joining Technologies for New Materials II" (AWS, Miami, FL, 1994) pp. 76–88.
8. T. J. MOORE and J. M. KALINOWSKI, *MRS Symp. Proc.* **288** (1993) 1173.
9. E. F. NIPPES (ed.), "Metals Handbook", Vol. **6** (ASM, Materials park, OH, 1983).
10. G. E. SHEWARD, "High Temperature Brazing in Controlled Atmospheres" (Pergamon Press, Oxford 1985).
11. S. V. OREL, L. C. PAROUS and W. F. GALE, *Weld. J.* (*Res. Suppl.*) **74** (1995) 3/95.
12. W. F. GALE and E. R. WALLACH, *Mater. Sci. Technol.* **7** (1991) 1143.
13. A. MISRA, R. D. NOEBE and R. GIBALA, *MRS Symp. Proc.* **288** (1993) 483.
14. M. LARSEN, A. MISRA, S. HARTFIELD-WUNSCH, R. NOEBE and R. GIBALA, *ibid.* **194** (1990) 191.
15. S. V. OREL, L. C. PAROUS and W. F. GALE, in "Proceedings of Advanced Joining Technologies for New Materials II" edited by N.F. Flore and J.O. Stiegler (AWS, Miami, FL, 1994) pp. 5–19.
16. VON J. D. SCHÖBEL and H. H. STADELMAIER, *Z. Metallkde* **56** (1965) 856.
17. G. PETZOW and G. EFFENBERG (eds), "Ternary Alloys, A Comprehensive Compendium of Evaluated Constitutional Data and Phase Diagrams" (VCH, New York, NY, 1991).
18. A. J. MARKHAM, PhD thesis, University of Cambridge, UK (1988).
19. W. F. GALE and E. R. WALLACH, *Metall. Trans.* **22A** (1991) 2451.

Received 12 January
and accepted 22 June 1995